Thesis for the degree of Master of Science

Facile synthesis of rare earth metal Vanadate Neodymium Vanadate anchored on GQD decorated Silver Nanowire for Efficient Electrochemical Water splitting

The Graduate School

Of the University of Ulsan

Department of Chemical Engineering and Bioengineering

Srushtee Sanjay Bhosale

Facile synthesis of rare earth metal Vanadate Neodymium Vanadate anchored on GQD decorated Silver Nanowire for Efficient Electrochemical Water splitting

Supervisor: Prof. Won Mook Choi

A Dissertation

Submitted to
The Graduate School of the University of Ulsan
2023

By
Srushtee Sanjay Bhosale

Department of Chemical Engineering and BioengineeringUniversity of Ulsan, Korea
February 2023

Facile synthesis of rare earth metal Vanadate Neodymium Vanadate anchored on GQD decorated Silver Nanowire for Efficient Electrochemical Water splitting

This certifies that the master's thesis of

Srushtee Sanjay Bhosale is approved.

Committee Chair Prof. Hur Seung Hyun

Committee Member Prof. Kang Sung Gu

Committee Member Prof. Choi Won Mook

Department of Chemical Engineering and Bioengineering

University of Ulsan, Korea

February 2024

ABSTRACT

In this work we synthesized the Neodymium Vanadate anchored on GQD decorated silver nanowire for electrochemical water splitting HER and OER. The composite was prepared through simple hydrothermal method and investigated the composite's structural and catalytic qualities. The AgNW@ GQD gave the entire composite a larger surface area and greater structural stability. To generate 50mA cm^{-2} current density and a low Tafel slope value of 107 mV/dec^{-1}, $NdVO_4$/AgNW@GQD requires 267 mV of overpotential which is low compared to $NdVO_4$, AgNW @GQD and commercial Pt/C electrode. Additionally, composite was used as an anode material in the OER reaction; however, 150 mV (vs RHE) overpotential was required to produce the current density of 10 mA cm^{-2} current density, while the tafel slope value is 131 mV/dec^{-1} .In the long-term chronoamperometric investigation, the current density for HER and OER increased up to 87% and 92%, respectively, over 100 hours, with nearly no changes.

Keywords: $NdVO_4$, AgNW@GQD, Water splitting, Electrocatalyst, hydrogen evolution reaction

Table of Contents

2.4.1 Cathode Activity:Hydrogen Evolution Reaction (HER)

2.4.2 Oxygen Evolution Reaction activity (OER)

2.4.3 Stability Study of Composite

2.5 Conclusion

Chapter 1. Introduction

OVERVIEW

1.1.Need of Hydrogen generation

Modernity has a debt to energy consumption, and fossil fuel resources mostly meet the world's energy needs. The ongoing use of finite fossil fuel resources has changed perspectives on the world's energy needs in the absence of fossil fuels. The alarm of accelerated global warming in this regard causes the globe to turn its attention to clean and renewable energy sources[1]. The two fundamental concerns facing humanity today are the inevitable depletion of fossil fuel resources, which is being compounded by an increase in energy consumption, and the uncertain future of climate change [2]. These issues should be resolved by the creation of carbon-neutral energy systems in order to establish an environmentally friendly energy for the future of the planet[3]. One of the most intriguing alternative energy sources that does not occur naturally is hydrogen. Similar to how electricity is not a source of energy, hydrogen is also seen to be a secondary form of energy that is produced from natural and biological resources. According to predictions, hydrogen will play a significant part in the future of the energy sectors . With a density of 0.0695 in relation to air, hydrogen is the lightest element and a colorless, odorless, and tasteless gas.

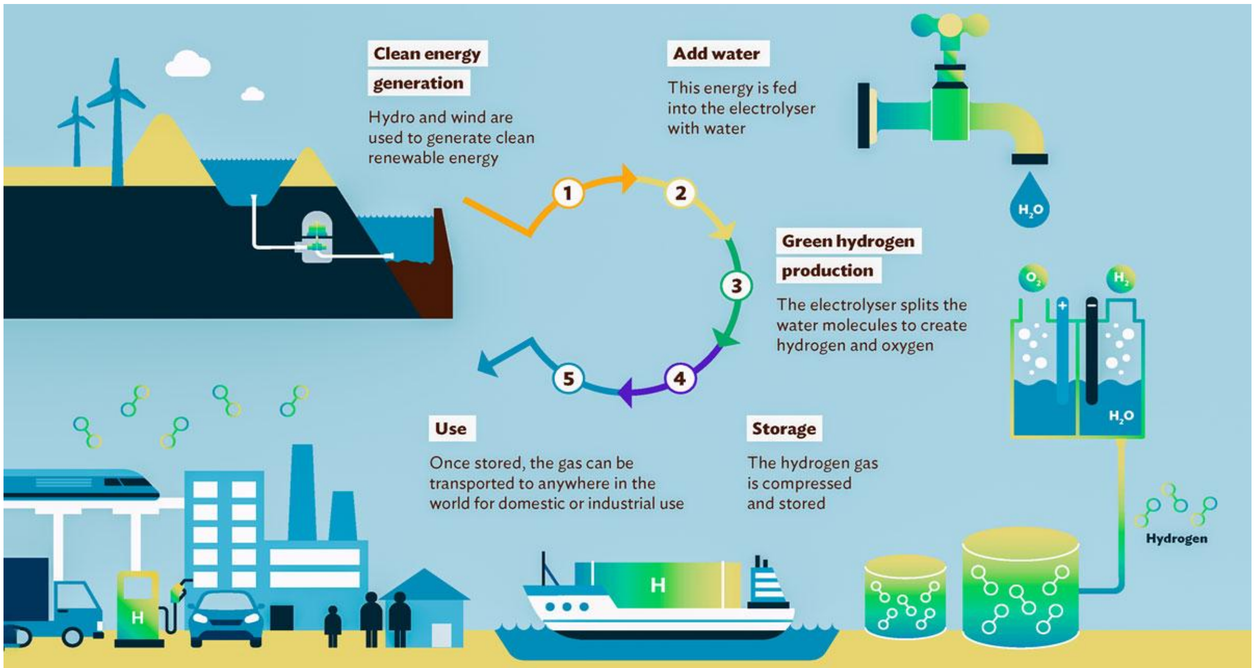

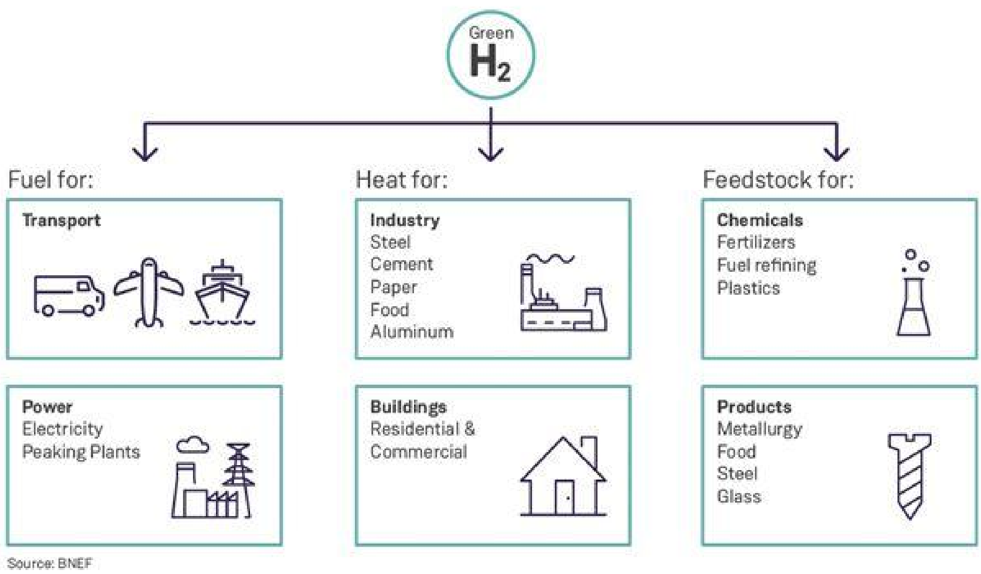

Schematic Figure.1. Green Hydrogen Energy Production cycle and Green Hydrogen uses

1.2.Hydrogen production from water electrolysis

Electrocatalytic water-splitting is one of the most ideal and effective ways to produce hydrogen with high purity. The watersplitting reaction is known with two half reactions: the water oxidation reaction (or oxygen evolution reaction, OER) and the water reduction reaction (or hydrogen evolution reaction, HER).

Total reaction: $2H_2O \longrightarrow O_2 + 2H_2$

Anode: $2H_2O \longrightarrow O_2 + 4e + 4H^*$ (OER)

Cathode: $4e + 4H^* \longrightarrow 2H_2$ (HER)

On the cathode the HER process generally involves three possible reaction steps as fallows:

(1) Volmer Reaction (Electrochemical hydrogen adsorption):

$H_3O^+ + M + e^- \longrightarrow M\text{-}H^* + H_2O$ (acidic medium)

$H_2O + M + e^- \longrightarrow M\text{-}H^* + OH^-$ (alkaline medium)

(2) Heyrovsky reaction (electrochemical desorption):

$H^+ + e^- + M\text{-}H^* \longrightarrow H_2 + M$ (acidic medium)

$H_2O + e^- + M\text{-}H^* \rightarrow H_2 + OH^- + M$ (alkaline medium)

(3) Tafel reaction (Chemical desorption):

$2M\text{-}H^* \rightarrow H_2 + 2M$ (both acidic and alkaline media)

The experimental information on Tafel slope aids in assuming the reaction's mechanism. A suitable catalyst that would reduce the activation energy and overpotential is required for the HER process. Due to their longevity over time and nearly zero over potential, platinum (Pt), in particular its 111 facets, is a commonly utilized catalyst for HER.

However, because of their high cost and scarcity, HER catalysts had to be replaced. Additionally, the hydroxyl ion poisoning of the Pt catalyst surface restricts its use in alkaline media,necessitating the replacement of Pt catalyst with high stability and low overpotential

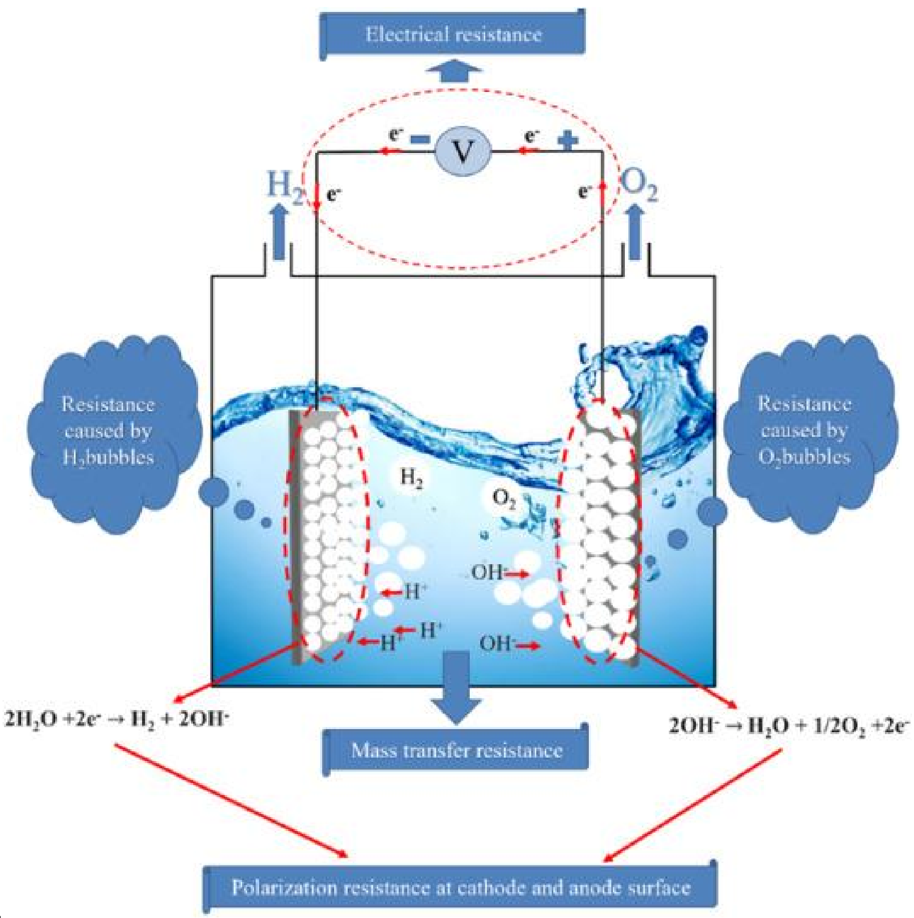

[4].

Schematic Figure 2.Representation of Energy related applications in fuel cell, Oxygen Evolution Reaction (OER) and Hydrogen Evolution reaction (HER) by water hydrolysis.

1.3. Introduction of Materials:-

Neodymium Vanadate ($NdVO_4$)

NdVO4 is a member of the D194h space group of zircon and is a rare earth vanadate. It forms a tetragonal structure during crystallization, with rare earth ions Nd3+ sandwiched in between the neighboring VO3-4 tetrahedra. Eight oxygen ions form a dodecahedron around each Nd3+ ion. Functionalized nanoparticles can be added to improve electrochemical performance. A larger conductivity and detection range are made possible by the surface change, which accelerates electron transport kinetics.

In order to create intelligent, portable, compact, and advanced catalyst, it is necessary to develop biocompatible, economical, and energy-efficient alternatives. It is difficult to create advanced functional nanomaterials with widespread application because of problems with their development. The majority of the materials on the market give up on qualities including safety, scalability, longevity, selectivity, and recovery.One potential class of nanomaterials used for the detection of environmental contaminants is rare earth vanadates (RVO4, R = cations). Good electrochemical foundations are made possible by their outstanding structural stability, tunable bandgaps, strong ionic conductivity, low charge transfer resistance, many oxygen vacancies, and quick electron-hole recombination. Neodymium vanadate ($NdVO_4$) is a particularly popular photocatalytic and semiconducting material owing to its good optical, electrical, and photochemical properties.46 Assimilating the unique features of 4 f electron transitions of Nd3+, neodymium vanadates (NdVO4) show appreciable physical and chemical properties.47 The charge distribution between Nd3+ and zircon-type tetragonal VO4 3− is significant of its electrochemical activity. The wide bandgap (>3 eV) and the presence ofsufficient charge carriers enable NdVO4 to demonstrate significant redox capacity toward targeted contaminants.

Unsupported electrode materials are, however, susceptible to additional growth and flaking during redox reactions, resulting in diminished stability and efficacy. Several strategies with conductive carbonaceous materials for enhancing electrode efficiency have been proposed in the literature. Molecular confinement in nanopores is a major assistance for such porous nanostructures. Doping carbon nanostructures with the main material enhances porosity and assists in tuning the surface morphology, chemical properties, and electron transportation. The defects induced by the dopant can advance charge transfer, resulting in higher redox current. Employing carbon based nanomaterials as a dopant obliges as an economic and non-toxic strategy when compared to most of the other known dopants routinely adopted.

Silver Nanowire

Silver nanowires can serve as a support material for other catalysts like platinum or ruthenium, which are commonly used for the HER and OER. These nanowires can offer structural support and help in the dispersion of the catalyst material, leading to better catalytic performance.

Silver nanowires can provide a high surface area and good electrical conductivity, making them efficient for catalyzing these reactions. They can serve as the support for other catalyst materials, such as metal oxides, to enhance the overall electrocatalytic activity.

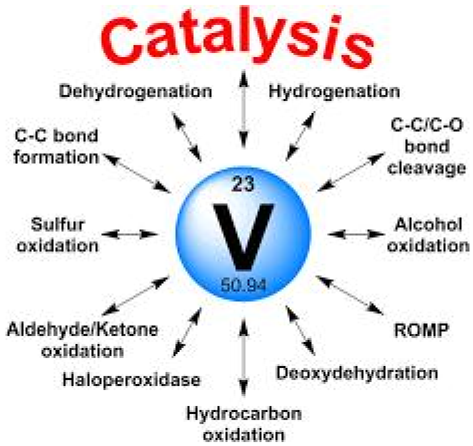

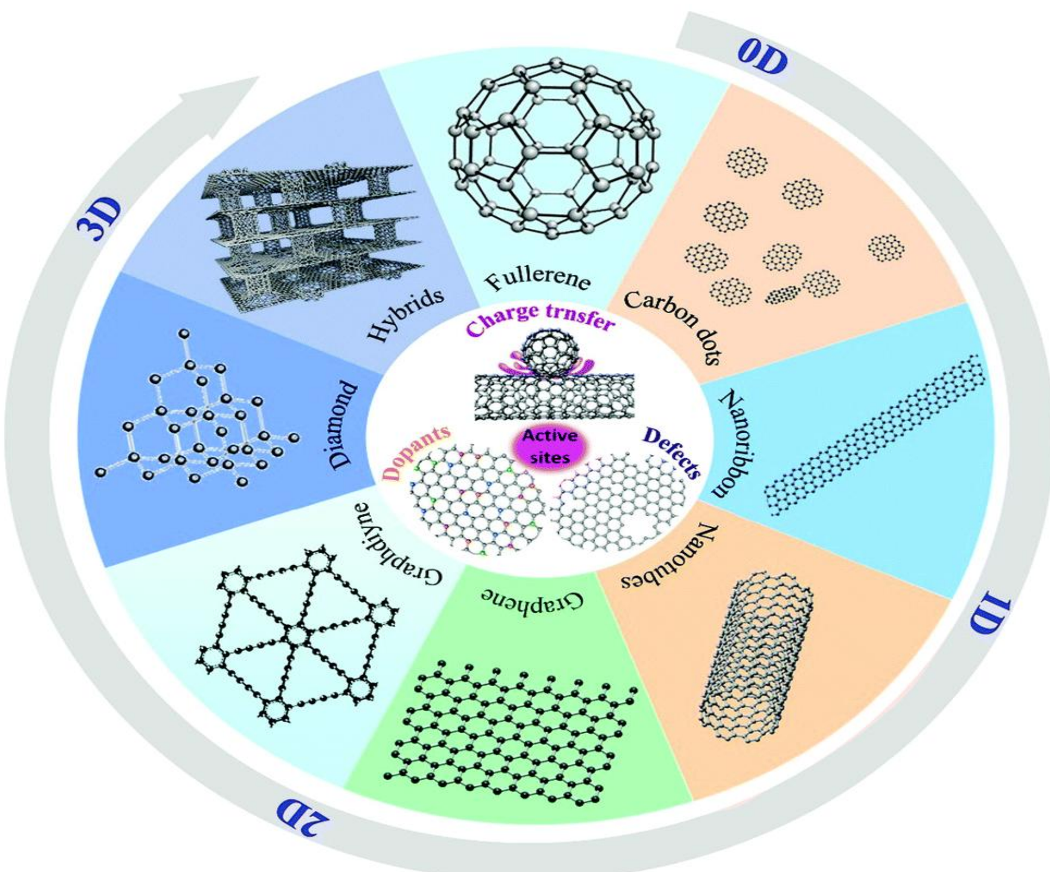

Schematic Fig.2. Vanadium working as a catalyst and Carbon Nanomaterials used in catalyst

CHAPTER 2.Synthesis of novel rare metal Vanadate Neodymium Vanadate anchored on GQD decorated Silver Nanowire for Efficient Electrochemical Water splitting

2.1 Introduction

The use of hydrogen (H_2) spans a wide range of industries, from the creation of methanol and ammonia in factories to the production of semiconductors and the refining of petroleum. Increasing need for clean and renewable energy sources has created a new opportunity for effectively using hydrogen. As a safe and practical way to produce hydrogen, electrochemical water splitting (EWS), which runs in a controlled environment and is powered by electricity, has received praise. Alternative energy. Two people are involved in electrochemical water splitting, Hydrogen evolution reaction (HER) on the other hand, is one of the oxygen evolution reaction (OER) on the anode and the cathode.

$NdVO_4$ powders have been investigated for their photocatalytic activity. They can be used in the degradation of organic pollutants and as photocatalysts in various photochemical reactions. It can promote or accelerate the rate of chemical reactions without being consumed in the process. $NdVO_4$ is a member of the D19 4h space group zircon structure. It forms a tetragonal structure during crystallization, with rare earth ions Nd^{3+} sandwiched between the neighboring VO^{3-4} tetrahedra. In the photocatalytic reaction, the regular VO_4 tetrahedra and Nd^{3+} of $NdVO_4$ are essential components.

The synthesis of $NdVO_4$ nanoparticles using different wet chemical methods, such as the citrate method[1]and the hydrothermal method[2], allows for the creation of nanomaterials with specific properties and structures. These studies represent examples of how wet chemical methods can be used to tailor the properties and structures of $NdVO_4$ nanoparticles for specific applications. The choice of synthesis method, along with the conditions and precursors used, can have a significant impact on the resulting material's characteristics and performance.

In contrast, to successfully reduce the oxidation of AgNPs, a protective coating on their surface is recommended. The covering layer actually serves two purposes. One advantage is that it can prevent AgNPs aggregation. On the other side, it will also prevent interaction with oxygen, reducing AgNPs' oxidation. When heated electrons in silver (Ag) are excited from the valence band (VB) to the conduction band (CB), localized surface plasmon states are produced. These energized charge carriers, in the form of photogenerated electrons and holes, play a pivotal role in initiating redox reactions. When we evaluate plasmonic metals like gold (Au), silver (Ag), and copper (Cu) in the context of photoelectrochemical (PEC) water splitting, it becomes evident that silver (Ag) stands out due to its remarkable electrical conductivity. This high electrical conductivity enables Ag to excel in the generation of charge carriers while effectively mitigating the recombination rate, making it particularly beneficial for PEC water splitting processes.

2.2 Experimental

2.2.1. Chemicals and Instruments

X-Ray diffraction analysis was conducted utilizing a ULTIMA 4 X-ray diffractometer and monochromatic Cu radiation with a wavelength of 0.154 nm, an X-ray diffraction (XRD) examination was carried out. 30 minutes were allotted for each sample, and the scanning rate was set at 2 min, spanning a range of 10 to 90 degrees. A K alpha model was used for X-ray photoelectron spectroscopy (X-Ray, 400um, Thermo Fisher). Utilizing an energy-dispersive X-ray spectrometer (EDX) and a field emission scanning electron microscope for elemental analysis, the morphologies of the catalyst surfaces were examined. For samples that were coarsely powdered, Raman peaks were recorded using a DXRTM3 Raman Microscope (Thermo Fisher Scientific). A Nicolet iS5 spectrometer was used to perform FT-IR data.

2.2.2 Synthesis of $NdVO_4$/AgNW@GQD

Neodymium Vanadate nanostructures were synthesized in the presence of PVP as a surfactant during a straight forward hydrothermal process to create neodymium vanadate nanostructures.Initially, 30 ml of deionized water was dissolved with 0.2 g of Nd $(NO_3)_3$–6H2O. The a forementioned solution was then mixed with 0.05 g of NH_4VO_3 solution in 30 ml of deionized water at 60 °C. Nd:V is stoichiometrically 1:1 for each sample.. The solution containing neodymium and vanadium was stirred for 10 min each, after which 0.5g PVP 30 was added in above solution, and again stirred for 1h. The pH of suspension was adjusted using NaOH to pH 4. Transfer the prepared solution to Teflon lined autoclave and kept in muffle furnace for 12h at 180 °C.Neodymium vanadate powder was centrifuged after being repeatedly cleaned with ethanol and water. The yellowish green precipitate was calcined at 400 °C for 4 hours in an air environment after being dried up at 60 °C overnight. For preparing AgNW@GQD suspension 1:1 ratio of AgNW and GOD was taken. The suspended mixture was then probe sonicated for 1hr and used for preparing composite. $NdVO_4$ powder and AgNW@GQD suspension were combined in a 1:1 ratio to create the composite (2 mg of $NdVO_4$ powder and 200 ul of AgNW@GQD).

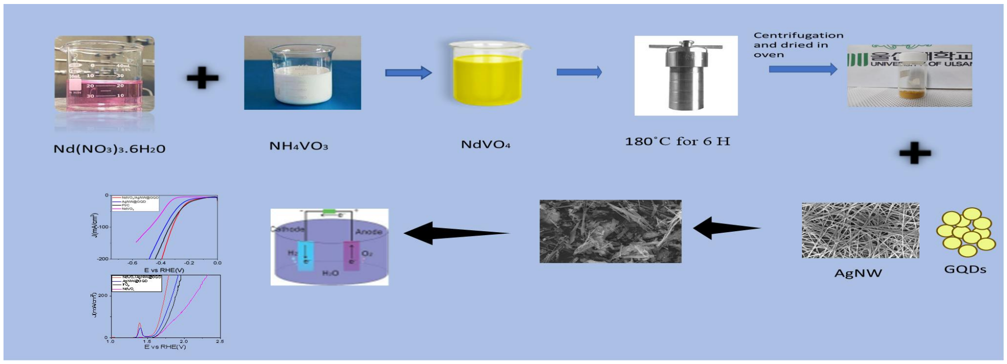

Schematic Fig.1. Synthesis of $NdVO_4$ and $NdVO_4$ /AgNW@GQD for Water splitting

2.3. Results and Discussion

2.3.1 XRD Analysis

Powder XRD patterns are used to assess the phase's crystallinity and purity produced NdVO4 samples. The diffraction peaks in Fig. 1 (A) can be attributed to $NdVO_4$'s tetragonal phase (JCPDS 15-0769; space group: 141/ amd). The detected diffraction peaks correspond to the orientation planes of (200), (112), (220), (301), (103), (321), (312), (400), (420), (332),(422) and (224) and are located at 24.27, 32.69, 34.63, 39.52, 46.86, 48.44, 49.79, 56.08, 60.83, 63.10, and 68.67, respectively. The well-crystalline single-phase development of $NdVO_4$ was revealed by the XRD pattern. however minor impurities can be observed. For AgNW@GQD the corresponding peaks come at 38.115, 44.299, 64.443, 77.397 correspond to (111), (200),(220), (311), respectively. These are in accordance with the JCPDS no. (01-087-0597). For GQD the carbon peaks come at 26.611, 43.455 correspond to (111), (010), respectively. The diffraction peaks for NdVO4, AgNW, GQD confirms the successful formation of hybrid composite NdVO4/AgNW @GQD.

2.3.2 RAMAN Spectra Analysis

$NdVO_4$ sample Raman spectra were measured between 500 and 1100 cm^{-1} (Fig. 1(B)). The presence of vanadate ions is confirmed in all samples by the Raman peaks that were seen around 770 cm^{-1} and 876 cm^{-1}. The metal oxygen-bonds -O-V-O-'s symmetric stretching mode is represented by the conspicuous Raman peak at 876 cm^{-1}. The observed Raman Peaks around 278 cm^{-1} and 301 cm^{-1} confirms B1g external modes of vibrations, similarly the peaks at 473cm^{-1} and 527cm^{-1} corresponds to B1g (V_4) type of internal vibration mode. The peaks at 398cm^{-1} and 863cm^{-1} correspond to A1g vibrations in internal modes. The peak at 139cm^{-1} is the only Eg mode which can be present as interlayer shear modes. In the AgNW@ GQD the disorder in carbon is what is responsible for the D band peak (1380 cm^{-1}). The breathing mode with an A1g symmetric molecular orbital is visible in the D peak. The G band peak (1570 cm1) is attributed to sp2-hybridized carbon with E2g symmetry's phonon vibration, according to studies. The narrow D and G bands demonstrate that graphene sheets are present in both samples. In the composite the D and G bands are slightly blue shifted which D peak to (1370cm^{-1}) and G peak to (1560cm^{-1}). In AgNW @GQD the peaks at 1070cm^{-1} indicate V[C-C]. Raman spectroscopy blue shifts can result from a number of things, such as modifications to the sample's chemical environment, modifications to its molecular structure, or interactions with nearby molecules.

2.3.3 FT-IR Analysis

The stretching vibration of the hydrogen-bonded OH groups of the adsorbed water is responsible for the absorption in the range of 3000 to 3600 cm^{-1}. The absorption band at 1034 cm^{-1} is attributable to the C-N stretching vibration, while the VO_4 stretching vibration and V-O bond have been seen at 443 cm^{-1} and 791 cm^{-1}, respectively. As demonstrated in Fig. 1(C), the bending OH groups in water that are hydrogen-bonded vibrate can be attributed to the adsorption at a distance of 1631 cm^{-1}. The band at 444 cm^{-1} is associated with the stretching vibration of VO_4. V-O bond causes a band at 793 cm^{-1}. A faint band at 1539 cm^{-1} is depicted in Fig. 1(C) and is associated with aromatic C-H stretching in AgNW@GQD and Composite. AgNW@GQD also exhibits a band at 1014 cm^{-1} and 1019 cm^{-1} that corresponds to C-N stretching, respectively, as well as a faint band at 1246 cm^{-1} that denotes the presence of N-H stretching on both surfaces. The aforementioned bands show that $NdVO_4$ and AgNWs-GQD surfaces still have both C-N and N-H functional groups present.

2.3.4XPS Analysis

Peaks in the banded energy Nd^0 $3d_{5/2}$, Nd^0 $3d_{3/2}$, Nd^{3+} $3d_{5/2}$, and Nd^{3+} $3d_{3/2}$ may be assigned to Fig.2.(B) at around 975 eV, 1002 eV, 981 eV, and 1005 eV, respectively. The peaks at approximately 515 eV, 517 eV, 524 eV, and 525 eV, respectively, corresponded to V^{4+} $2p_{3/2}$, V^{5+} $2p_{3/2}$, V^{4+} $2p_{1/2}$, and V^{4+} $2p_{1/2}$.. The peaks atFig.3(C) about 528 eV and 534 eV were 1s characteristic peaks for lattice oxygen and adsorbed oxygen. $3d_{5/2}$ and $3d_{3/2}$ peaks for silver come around 366 eV and 372eV. And from Fig.2.(F) the observed peaks for C 1s in AgNW @GQD are 286eV, 287eV(C-C) and 289 eV(C-OH)bonds respectively. In composite the C 1s peaks are slightly shifted to low binding energy 283eV(C-C) and 285eV(C-OH). This blue shift shows the surface interaction between $NdVO_4$ and AgNW @GQD. Similarly Nd peaks in composite also show blue shift and the new peaks come at 978eV, 981eV, 989eV and 992eV for Nd^0 $3d_{5/2}$, Nd^0 $3d_{3/2}$, Nd^{3+} $3d_{5/2}$ and Nd^{3+} $3d_{3/2}$. In Fig.2. V 2p in the composite also has blue shift in the peaks that means the surface kinetics affects the oxidation peaks of composite and the V 2p peaks are shifted to 513eV, 515eV, 522eV and 524eV respectively.

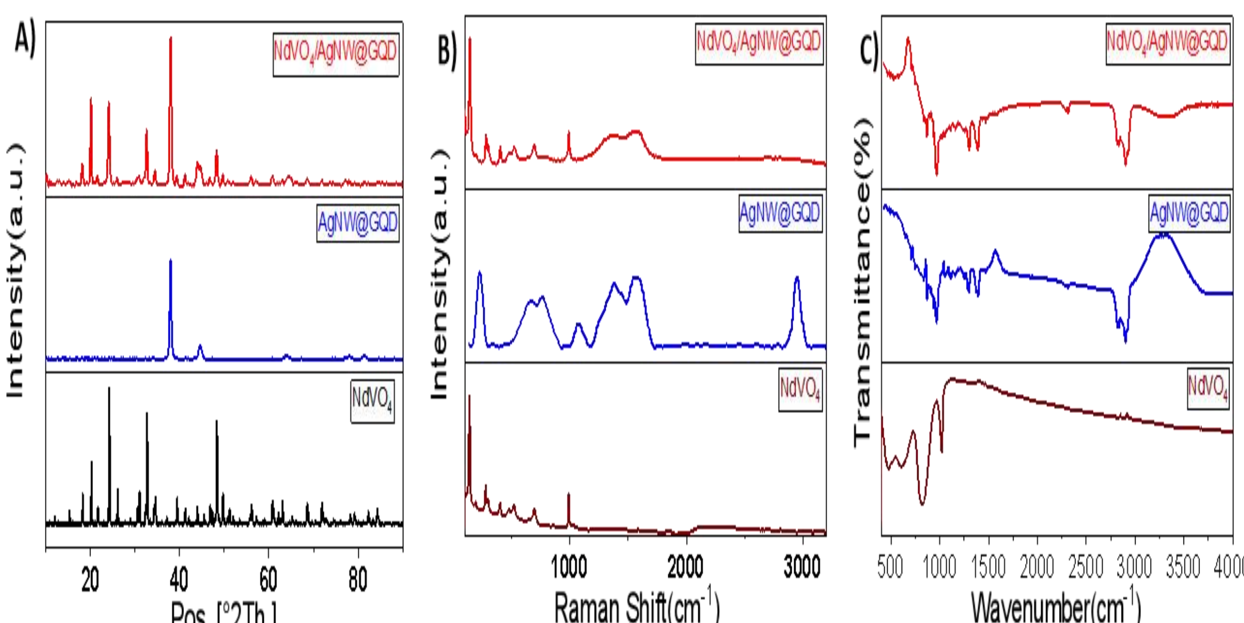

Fig.1, A) XRD pattern of $NdVO_4$, AgNW @GQD, $NdVO_4$/AgNW @GQD B) Raman Spectra, $NdVO_4$, AgNW @GQD, $NdVO_4$/AgNW @GQD C) FT-IR of $NdVO_4$, AgNW @GQD, $NdVO_4$/AgNW @GQD

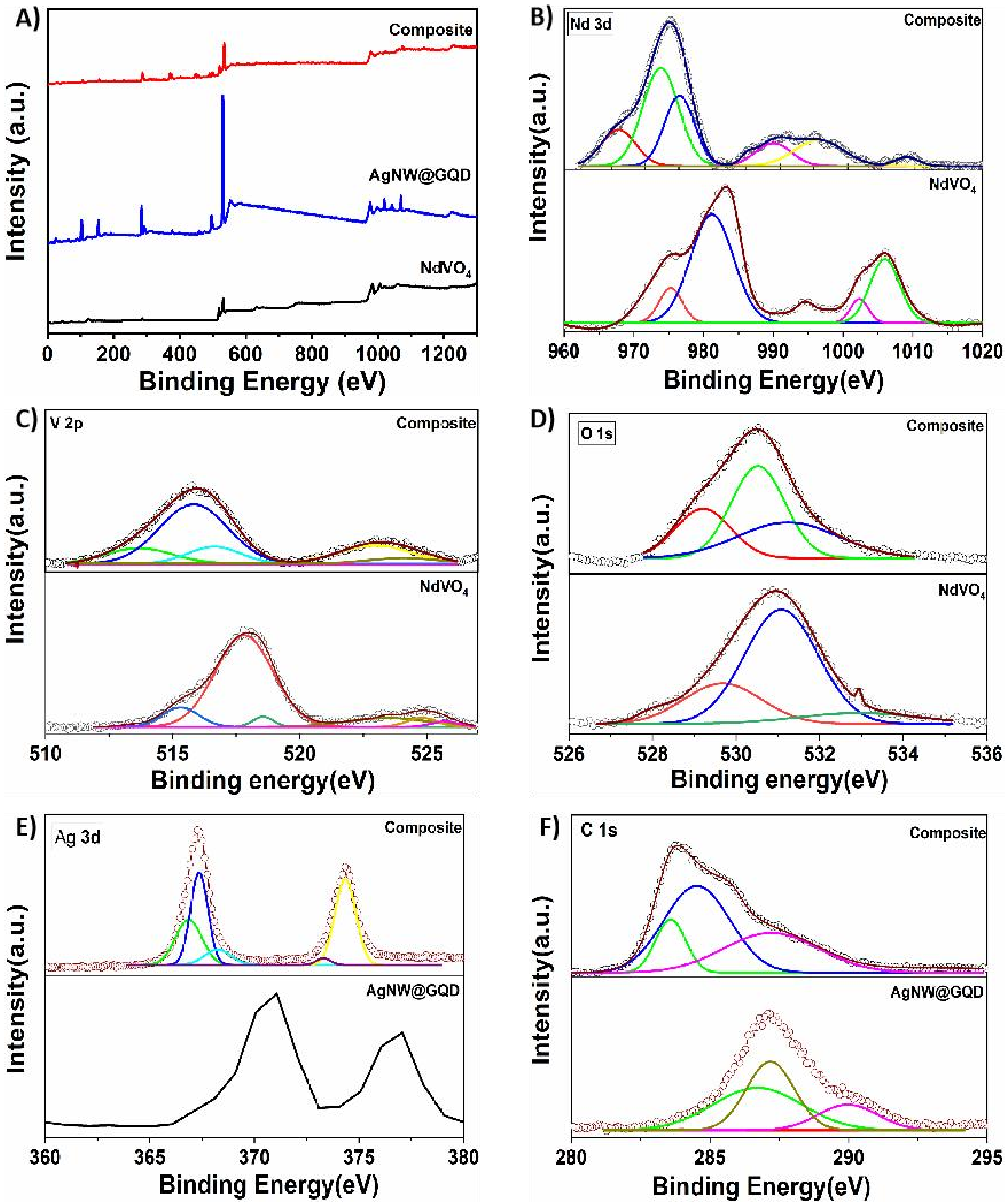

Fig 2. Elemental XPS Analysis A) Survey spectrum B) Nd 3d, C) V 2p, D) O 1s, E) Ag 3d,

F) C 1s, respectively.

2.4 Electrochemical Water splitting performance

2.4.1. Cathode Activity: Hydrogen Evolution Reaction

The catalytic activity of the as-synthesized $NdVO_4$/AgNW@ GQD material were monitored using 1.0 M KOH solution. The catalytic activities of NdVO4, AgNW@ GQD were examined concurrently with the composite NdVO4/AgNW@ GQD in order to comprehend the contributions of each component included in the composite.Drop casting was used to apply the produced materials to clean NF (nanofiber) substrates, which served as the working electrode. In

materials science and electrochemistry, a technique known as drop-casting is frequently used to deposit a solution or suspension of a material onto a substrate by allowing droplets to fall to the surface. A good catalyst in electrocatalysis is one that can achieve a high current density (more product generated) with a low overpotential (less extra energy required). This means it can produce more product with lower energy input, making it more efficient and effective in the electrochemical reaction. As shown in fig the $NdVO_4$/AgNW@ GQD showed a higher activity regarding overpotential of 267 mV to achieve 50mA cm-2 current density over NdVO4(386mV), and AgNW@ GQD(301mV). Even lower than that of commercial Pt/C (270mV), the composite has the lowest overpotential to generate 50 mA cm2 current density (50=267mV). Although it is nearly close to commercial Pt/C but as the overpotential increases the current density of the composite is stable and higher than that of commercial Pt/C. The NdVO4/AgNW@ GQD among all synthesized materials has the highest mass activity value (), which is also consistent with its highest current density. Studying current densities at constant potentials, such as 100 mV and 200 mV, revealed that among the produced compounds, composite had a greater current density. Tafel slope can be used to examine the rate of rise in current density by 10 units.

The Tafel slope is indeed an important parameter in determining the rate of electrochemical reactions, including the Hydrogen Evolution Reaction (HER). It provides valuable information about the reaction kinetics and the mechanism of the reaction. The Tafel slope is a measure of how the reaction rate changes with changes in the overpotential (the deviation of the electrode potential from its equilibrium value). In the context of the HER, it relates the overpotential (η) to the reaction rate (i), and it can be expressed as:

Tafel slope (b) = $d(\log i) / d(\eta)$

In simpler terms, the Tafel slope quantifies how the logarithm of the reaction rate varies with changes in overpotential. The Tafel slope can be used to deduce information about the reaction mechanism because different mechanisms will result in different Tafel slopes.

A Tafel slope of around 120 mV/decade is often associated with the Volmer-Heyrovsky-Tafel mechanism for the HER, which involves a series of steps including the adsorption of hydrogen ions and the subsequent reduction to form hydrogen gas. A Tafel slope significantly different from this value could indicate a different rate-determining step and, therefore, a different reaction mechanism.

The exchange current density (J0) is a crucial parameter for assessing the electrocatalytic activity of a catalyst in electrochemical reactions. The exchange current density is the current density at which the net forward and reverse reactions of the electrochemical process occur at the same rate when the overpotential (η) is zero.

The expression you mentioned, $\eta 0 = b * \log(J0) + a$, relates the overpotential (η0) to the exchange current density (J0). The Tafel slope (b) and the constant (a) are parameters in this equation. As you correctly stated, lower J0 values indicate higher electron transfer rates and lower activation energy for the electrochemical reaction.

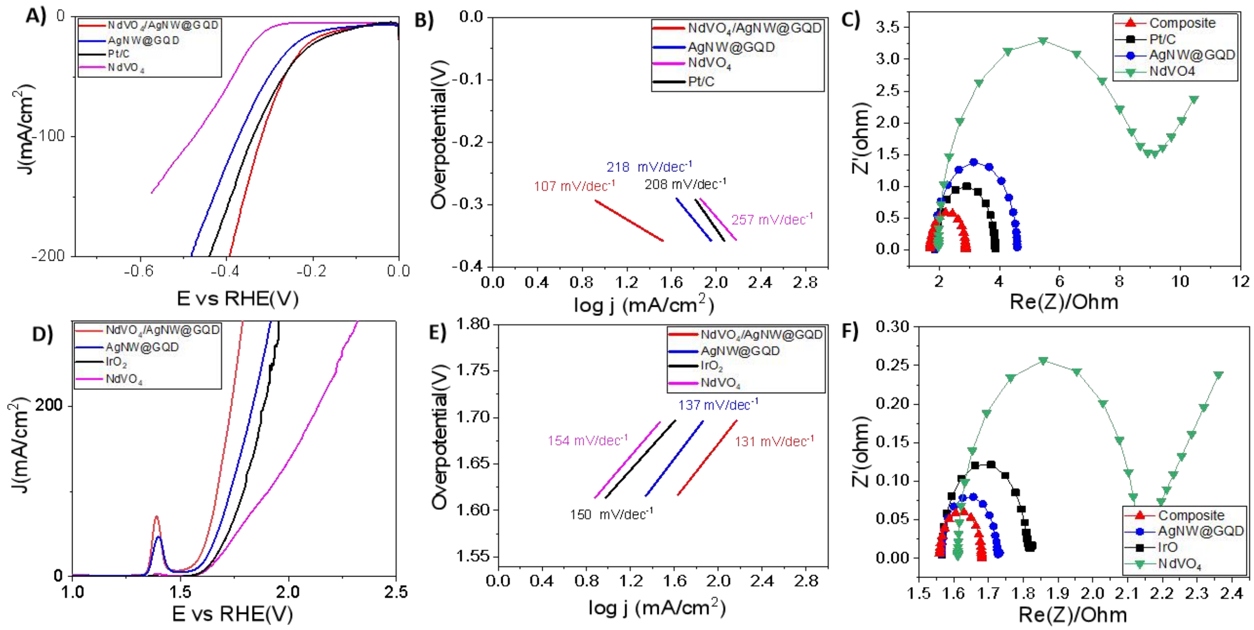

Fig .3. Catalytic Activities for cathode reactions HER and OER (A to D)Polarization curves , (B and E) Tafel Slopes, (C and F) Nyquist Plots of synthesized materials in 1M KOH electrolyte. Scan rate=5 mV/s

Materials	**η10**	**η50**	**η100**	**b mV dec-1**	**RCTΩ**	**J_0 mA/cm2**
NdVO4	**-0.3055**	**-0.3863**	**-0.4769**	**257**	**7.048**	**1.204**
AgNW@GQD	**-0.1834**	**-0.3014**	**-0.3732**	**218**	**2.759**	**1.229**
Composite	**-0.127**	**-0.267**	**-0.3194**	**107**	**1.184**	**2.774**
Pt/C	**-0.1036**	**-0.2740**	**-0.3393**	**208**	**2.009**	**2.264**

Table No.1 Activities of the materials toward hydrogen evolution reaction in 0.1M KOH

For understanding the inherent catalytic behavior of electrocatalysts, the idea of specific activity (SA) is fundamental. Specific activity is commonly represented as SA = J / (m * ECSA), where SA is the current density (J) normalized by the mass loading of the catalyst on the electrode surface (m) and the electrochemical active surface area (ECSA).

J is the current density, which represents the rate of the electrochemical reaction.

- m is the mass loading of the catalyst on the electrode surface, indicating the amount of catalyst present.
- ECSA (electrochemical active surface area) is the area of the catalyst surface that actively participates in the electrochemical reaction. It involves the adsorption of reactants, intermediates, or products during the electrochemical process.

The ECSA results show that NdVO4/AgNW@GQD has higher SA at a certain potential indicating higher activity. Composite has high Cdlvalue(18.218) which means the number of active sites are more compared to NdVO4 and AgNW@GQD which has Cdl values of 11.830 and 10.343

A high Cdl value does indeed indicate that there are more active sites on the electrode surface. Active sites are locations on the electrode where electrochemical reactions can occur, and they play a critical role in catalyzing various electrochemical processes. These active sites can facilitate electron transfer and influence the kinetics of reactions, making them important for many electrocatalytic and electrochemical applications.

Electrochemical Impedance Spectroscopy (EIS) analysis can be used to evaluate and comprehend the efficiency of electron transfer on an electrode surface. EIS is a powerful electrochemical technique used to study the electrical behavior of electrochemical systems, and it provides valuable information about the electrode processes, including electron transfer efficiency. The charge transfer resistance (R_ct) at the electrode-electrolyte interface can be determined using spectroscopy (EIS), which measures the diameter of the semicircle in the Nyquist plot from high to low frequency.. A lower value of R_ct (indicated by a smaller semicircle diameter) is indicative of faster charge transfer and more facile catalysis. That means the electrochemical reaction at the electrode-electrolyte interface is proceeding more efficiently, which is often desirable in electrocatalysis and electrochemical processes. Table states that the NdVO4/AgnW@GQDposses lower Rctvalue(1.184) than the other materials with Pt/C having Rct value of 208. This proves that the electron transfer efficiency can be improved by the synergistic interaction of the metal phases, the metal phases work together in a way that enhances their overall performance, often improving their catalytic properties.

2.4.2. Oxygen Evolution Reaction Activity:

NdVO4/AgNW@GQD delivered 150 mV overpotential (10) to achieve the current density of 10 mA cm^{-2}, while commercial IrO2 had a 165 mV overpotential, as illustrated in those figures. The Tafel slope is a measure of the rate at which the current density (i) changes with the overpotential (η) in an electrochemical reaction. It provides insights into the mechanism of the reaction. Tafel slope value can be seen in the table(2).

The Tafel slope (b) is indeed related to the transfer coefficient (α) and can provide information about the rate-determining step (RDS) in an electrochemical reaction. The relationship between the Tafel slope and the transfer coefficient can be expressed as:

$$b = (2.303 * RT) / (F * \alpha)$$

Materials	η_{10}	η_{50}	η_{100}	b mV dec^{-1}	RCTΩ	J_0mA/cm^2
NdVO4	**1.6322**	**1.7588**	**1.9089**	**154**	**5.4536**	**0.1438**
AgNW@GQD	**1.5784**	**1.6697**	**1.7306**	**137**	**0.1544**	**0.1889**
Composite	**1.5077**	**1.6288**	**1.6752**	**131**	**0.1208**	**1.1521**
IrO2	**1.6521**	**1.7168**	**1.7918**	**150**	**0.2528**	**0.5047**

Table No.2 Activities of the materials toward oxygen evolution reaction in 0.1M KOH

Table No.2 Activities of the materials toward oxygen evolution reaction in 0.1M KOH

EIS analysis (Table .2) indicated that Composite particles (0.12 Ω) had lower resistance compared to NdVO4(5.4 Ω) and AgNW@GQD(0.15 Ω), thus it proves that the surface of composite shows more roughness compared to NdVO4 and AgNW@GQD.

2.4.3. Stability Study of Composite

For the electrode materials to be certified as competent, stability is also crucial.The stability of NdVO4 /AgNW@GQD was checked for over 100h through CA study, showing almost unaltered density. For both cathodic and anodic reactions, the chronoamperometric investigations were continued for a further 100 hours. The J versus t graph plots demonstrated that during alkaline HER, NdVO4/AgNW@GQD maintained 87% cathodic current density. The anodic current density of NdVO4/AgNW@GQD, on the other hand, was maintained at 92% during OER for 100 hours.

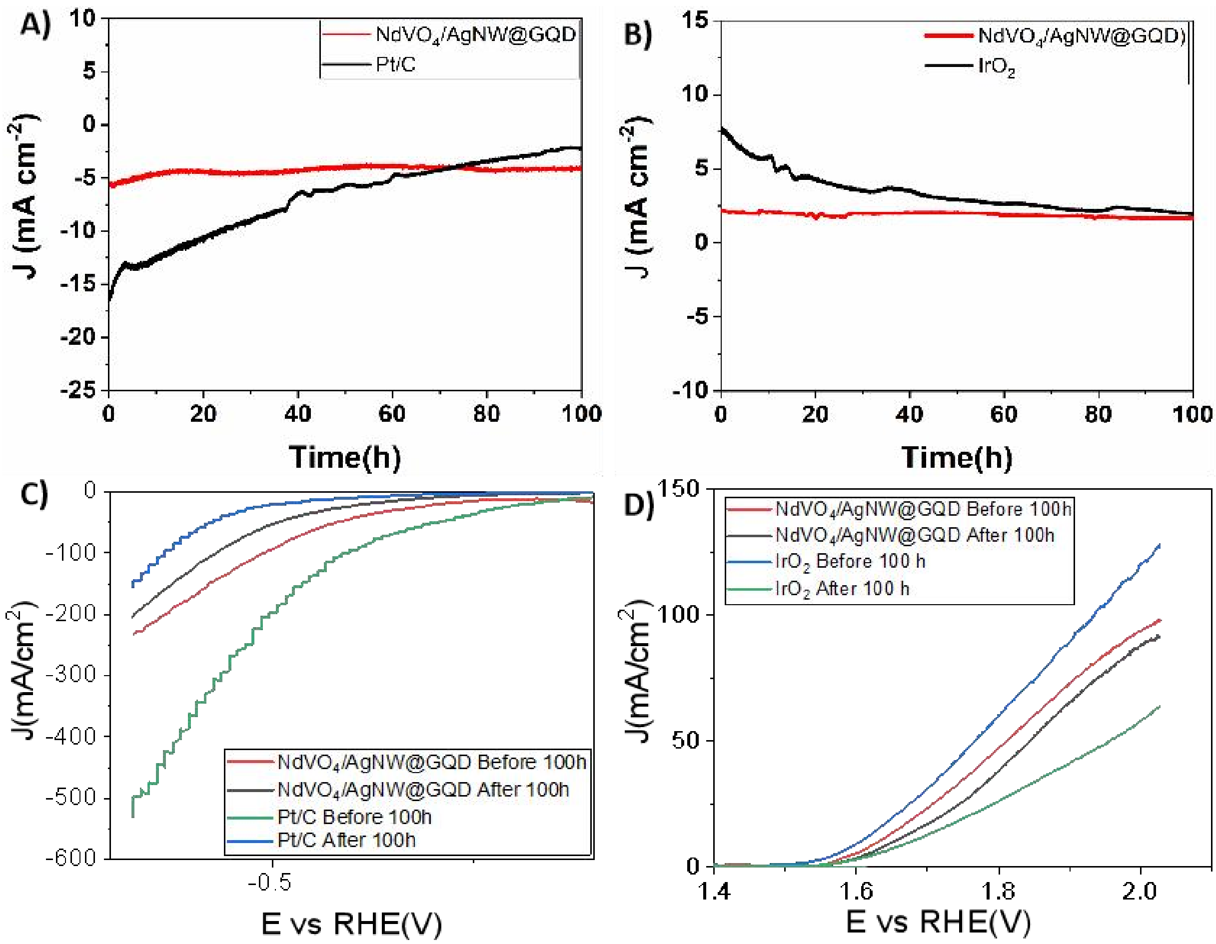

Fig.4. (A and B)Chronoamperometric study of $NdVO_4$/AgNW@GQD for 100 h HER and OER (C and D)Polarization curves Before and After 100 h cycle.

2.5. Conclusion

In this work we synthesized the Neodymium Vanadate anchored on GQD decorated Silver nanowire for electrochemical watersplitting HER and OER. The composite was made using a straightforward hydrothermal process, and its structural and catalytic properties were investigated. AgNW@GQD gave the entire composite a larger surface area and greater structural stability. To obtain 50mA cm-2 current density and a Tafel slope value of 131 mV/dec-1, NdVO4/AgNW@GQD required 267 mV. Additionally, a 150 mV (against RHE) overpotential was required to achieve a current density of 10 mA cm when composite was utilized as an anode material in an OER reaction. To the best of our knowledge, our work showed how NdVO4, AgNW, and GQDas can be combined to create an electrocatalyst for the first time. The multicomponent hetero-junction structure-based catalysts for HER and water splitting would benefit further from this work.

References:-

Deng, Y., Liu, H., Wei, X., Ding, L., Jiang, F., Cao, X., Zhou, Q., Xiang, M., Bai, J., & Gu, H. (2021). One-dimensional nitrogen-doped carbon frameworks embedded with zinc-cobalt nanoparticles for efficient overall water splitting. J Colloid Interface Sci, 585, 800-807. https://doi.org/10.1016/j.jcis.2020.10.060

P. Hajipour, A. Bahrami, M. Y. Mehr, W. D. van Driel and K. Zhang, Materials (Basel) 2021 Vol. 14 Issue 4 Accession Number: 33561955 PMCID: PMC7914779 DOI: 10.3390/ma14040763, https://www.ncbi.nlm.nih.gov/pubmed/33561955

Kim, T., Park, C., Kim, Y., Aldalbahi, A., El-Newehy, M., An, S., & Yoon, S. S. (2022). Enhancing Solar Radiant Heat Transfer Using Supersonically Sprayed rGO/AgNW Textured Surfaces. International Journal of Precision Engineering and Manufacturing-Green Technology, 10(1), 23-33. https://doi.org/10.1007/s40684-022-00431-1

Kim, T.-G., Park, C.-W., Woo, D.-Y., Choi, J., & Yoon, S. S. (2020). Efficient heat spreader using supersonically sprayed graphene and silver nanowire. Applied Thermal Engineering, 165. https://doi.org/10.1016/j.applthermaleng.2019.114572

Li, L., Wang, P., Shao, Q., & Huang, X. (2020). Metallic nanostructures with low dimensionality for electrochemical water splitting. Chem Soc Rev, 49(10), 3072-3106. https://doi.org/10.1039/d0cs00013b

Li, Y., Guan, S., Wang, R., & Li, Y. (2023). Low threshold photon avalanche upconversion emission for temperature sensing based on Yb(III)/Er(III) Co-doped NdVO4 with sphere 3D self-assembled structure microparticles. Ceramics International, 49(22), 35001-35010. https://doi.org/10.1016/j.ceramint.2023.08.174

Monsef, R., Ghiyasiyan-Arani, M., & Salavati-Niasari, M. (2018). Application of ultrasound-aided method for the synthesis of NdVO(4) nano-photocatalyst and investigation of eliminate dye in contaminant water. UltrasonSonochem, 42, 201-211. https://doi.org/10.1016/j.ultsonch.2017.11.025

Song, Y., Wang, R., Li, X., Shao, B., You, H., & He, C. (2022). Constructing a novel Ag nanowire@CeVO4 heterostructure photocatalyst for promoting charge separation and sunlight driven photodegradation of organic pollutants. Chinese Chemical Letters, 33(3), 1283-1287. https://doi.org/10.1016/j.cclet.2021.07.060

Sreedhar, A., Neelakanta Reddy, I., Ta, Q. T. H., Namgung, G., & Noh, J.-S. (2019). Plasmonic Ag nanowires sensitized ZnO flake-like structures as a potential photoanode material for enhanced visible light water splitting activity. Journal of Electroanalytical Chemistry, 832, 426-435. https://doi.org/10.1016/j.jelechem.2018.11.042

Yuvaraj, S., Kalai Selvan, R., Kumar, V. B., Perelshtein, I., Gedanken, A., Isakkimuthu, S., & Arumugam, S. (2014). Sonochemical synthesis, structural, magnetic and grain size dependent electrical properties of NdVO4 nanoparticles. UltrasonSonochem, 21(2), 599-605. https://doi.org/10.1016/j.ultsonch.2013.08.015

Jana, J., Nivetha, R., Diem, H. N., Van Phuc, T., Kang, S. G., Chung, J. S., Choi, W. M., & Hur, S. H. (2022). Improved kinetics of reduction of alkaline water on the g-CN- supported transition metal oxide/boride hetero-interface: A case study. International Journal of Energy Research, 46(11), 14979-14993. https://doi.org/10.1002/er.8198

Jana, J., Sharma, T. S. K., Chung, J. S., Choi, W. M., & Hur, S. H. (2023). The role of surface carbide/oxide heterojunction in electrocatalytic behavior of 3D-nanonest supported FeiMoj composites. Journal of Alloys and Compounds, 946. https://doi.org/10.1016/j.jallcom.2023.169395